Peer-reviewed version available at Appl. Sci. 2019, 9, 706; doi:10.3390/app9040706

Article

In-situ Monitoring and Analyzing Pitting Corrosion of Carbon Steel by Acoustic Emission

Junlei Tang [1], Junyang Li [2], Hu Wang [2,*], Yingying Wang [1], and Geng Chen [3]

[1] School of Chemistry and Chemical Engineering, Southwest Petroleum University, Chengdu 610500, China; tangjunlei@126.com (J. T.); yingyingwanglyon@126.com (Y.W.)
[2] School of Material Science and Engineering, Southwest Petroleum University, Chengdu 610500, China; 498881360@qq.com (J.L.); senty78@126.com (H. W.)
[3] CNOOC Energy Technology & Services-Shanghai Environmental Engineering & Technology Branch, Shanghai 200335,China; chengeng@cnooc.com.cn (G. C.)
* Correspondence: senty78@126.com (H.W.); Tel.: +86 028 83037361

Abstract: The acoustic emission (AE) technique was applied to monitor the pitting corrosion of carbon steel in $NaHCO_3$ + NaCl solutions. The open circuit potential (OCP) measurement and the corrosion morphology in-situ capturing using optical microscope were conducted during AE monitoring. The corrosion micromorphology was characterized with scanning electron microscope (SEM). The propagation behavior and AE features of natural pitting on carbon steel were investigated. After the performing of signal processing including pre-treatment, shape preserving interpolation and denoising for raw AE waveforms, three types of AE signals can be classified in the correlation diagrams of new waveform parameters. Finally, a 2D pattern recognition method was established to calculate the similarity of different continuous AE graphics, which is quite effective to distinguish the localized corrosion from uniform corrosion.

Keywords: carbon steel; pitting corrosion; acoustic emission; wavelets; pattern recognition

1. Introduction

In the modern construction industry, carbon steel is widely used because of low price and good mechanical properties. However, the corrosion resistance to aqueous environment of it is very low. Especially in the presence of saline medium, the probability of corrosion increases greatly, and most of them are localized corrosion. Structural damage and mechanical performance degradation can easily happen during long term service with localized corrosion. As one of the most destructive forms of localized corrosion, pitting corrosion of carbon steel intensively occurs in many sites, such as steel in reinforced concrete, steel with degraded coatings of bridge or water containment structure. Many investigations [1–3] have been done for the detection of structural failure of concrete with AE technique. As the initiation stage of many structural degradation cases, the pitting corrosion of carbon steel is essentially expected to be monitored.

It is commonly believed that pitting corrosion happens on more or less passivated metals and alloys in solution of halide ions [4]. The property of passive film plays an important role in the initiation, growth and re-passivation of pits. In most occasions, pitting process is regarded as several stages: 1) Local breakdown of passive film, represented as nucleation process, 2) Propagation (accelerated corrosion), 3) Stable growth, and (possibly) 4) Re-passivation. Stainless steels are typically passive initially [5]. The initiation of pitting is caused by adsorptions of halide ions through passive film. And the growth of pit undergoes mainly at the bottom as the anodic dissolution inside the pit. Cathodic reaction is nevertheless outside the pit, on inclusions or other defects. Stainless steels are relatively highly resistant to pit initiation, which can be ascribed to the excellent passivity of γ-Fe_2O_3 plus Cr_2O_3 oxide film at the surface. Hence, only limited amount of pits can be formed on

stainless steel surface. While whenever the pit forms, it often grows fast and develops in depth. The aggregation of corrosion products at the pit mouth accelerates the corrosion attack beneath the occluded area. The rupture or breakdown of the cover at pit mouth, including corrosion products and passive film, may result in the re-passivation, which implies the end of pitting corrosion. While as for other materials with less pronounced passive film, like carbon steels, pitting corrosion may start at inconsistent pores of passive film or corrosion products. Different from stainless steels, the growth of pitting undergoes in relatively slow rate. Pit may repeatedly experience the initiation-growth-re-passivation process [6]. In many occasions, the corrosion attack consists of many shallow pits in nearby area. The re-passivation of pit is most probably caused by the passivator in solution, not by the metal itself. The rupture or breakdown of passive film and product film is not as notable as stainless steel.

It is generally assumed that the iron oxide and ferrous bicarbonate can be formed as passive film of carbon steel in carbonate solution [5-6]. The origin of the passive film is from the oxidation of iron by dissolved oxygen and the deposition of insoluble ferrous bicarbonate. Many studies have focused on the structure and composition of passive film. Although there are two models of passive film (the γ-Fe_2O_3 layer and the γ-Fe_2O_3 plus Fe_3O_4 double layer), it is no doubt that the passive film on iron is mainly consisted of γ-Fe_2O_3. It is also more acceptable that the passive film of carbon steel in bicarbonate solution consists of inner Fe_3O_4 layer and outer γ-Fe_2O_3 layer, both combined with insoluble ferrous bicarbonate [5]. The inhomogeneity of passive film on carbon steel is the main reason for the initiation of pitting corrosion.

Many techniques have been used to study pitting corrosion. American Society for Testing and Materials (ASTM) has standardized methods for study/evaluation of pitting corrosion and pitting tests in 6% $FeCl_3$. Electrochemical measurements are most commonly used in investigating pitting corrosion behavior, e.g. polarization curves in measuring the break potential of pitting E_b, protective potential of pitting E_p, and the free corrosion potential E_{corr}. Current fluctuation behavior in potentiodynamic or potentiostatic polarization is extensively investigated to probe the metastable pitting, which is widely regarded as an important phenomenon before stable pitting and can be used to predict stable pitting events. Electrochemical impedance spectroscopy (EIS) is also widely used in the evaluation for the property of passive film under pitting attacking. Moreover, electrochemical noise (EN) is another useful technique in investigating pitting events and monitoring pitting corrosion. Although many approaches have been utilized in corrosion investigation, only limited techniques, like EN, linear polarization resistance probe [7-8], electrical resistance probe [9] and field signature technique [10], can be applied in pitting monitoring. All of them, however, have their limitations. For example, EN is quite sensitive in in-situ recording and identifying the initiation of pitting events [11-12]. But it is very difficult to interpret the data of propagation process. Therefore, in-situ monitoring and predicting pitting corrosion events in service is still a great challenge in industrial applications.

Acoustic emission (AE), an important technique which can be used in corrosion monitoring, has attracted great attentions in recent years. In most occasions, the happening of corrosion of metals and alloys is always accompanied by the rapid release of energy in the form of transient elastic wave. The nature of corrosion monitoring by AE is firstly built up of the relationship between corrosion attack and transient elastic wave. And such relationship is then used in in-situ monitoring the corrosion attack of material in service. AE is a non-destructive technique which aims at in-situ monitoring corrosion attack by detecting, recording and analyzing the acoustic emission signal. Modern AE technique began with the work of Kaiser in Germany in the last century, 1950s. In recent years, AE has been widely used in many applications, such as the petroleum and natural gas industry, aerospace industry, transportation industry and construction industry etc. [13-16].

Many types of corrosion have been studies by AE [17-25], such as stress corrosion cracking [18-20], abrasion or erosion corrosion [21], and pitting corrosion [22-25]. H. Mazille [22] proved that AE signals can be easily detected in pitting corrosion. Moreover, a good correlation between AE activity and pitting rate has been observed. Then, he and M. Fregonese et al. [23] studied the initiation and propagation of pitting corrosion on stainless steels with AE. They further demonstrated that the

initiation step of pitting corrosion was not significantly emissive, whereas the propagation step was characterized by the emission of resonant signals. They figured out the signals in the propagation step were ascribed to the evolution of hydrogen bubbles. More recent studies by other researchers, such as K. Darowicki had used AE and potentiodynamic methods to investigate the mechanism of pitting corrosion of stainless steel [24]. K. Wu and W.S. Jung used AE to monitor the pitting corrosion on vertically positioned 304 stainless steel, and analyzed the acoustic emission energy parameter[25]. However, most of the researchers used some methods such as potentiodynamic polarization, potentiostatic polarization or heater to accelerate the pitting corrosion of metals in a short time so that it could not be the real situation of the corrosion process of materials under natural conditions. The in-situ monitoring for pitting corrosion process under natural condition is very important to understand the corrosion behavior and perform the structural integrity management for steel construction.

The processing and analyzing of AE signal is the most important step in AE studies. In many studies, the acoustic emission signals are processed and classified by various methods, like K-means, random forest, wavelet analysis or some parameter analysis methods [26-33]. The application of some methods, for instance the K-means and random forest, only utilize some parameters of AE waveform (raw or pre-treated). The single use of wavelet only can optimize AE waveforms. Therefore, there are still a lot of work to do for developing the effective and integrative method to identify the corrosion type base on the raw data from the in-situ AE monitoring.

In this paper, the pitting corrosion of carbon steel was monitored by AE technique in $NaHCO_3$ + NaCl solutions. Open circuit potential experiments were carried out simultaneously to probe the relationship between AE and electrochemical behavior. In addition, the optical microscope was used to in-situ record the surface morphology of carbon steel under corrosion attacking in different conditions and SEM was used to observe the surface micromorphology after corrosion. Finally, Matlab was involved to establish the methods for AE data processing [33] and analyzing.

2. Materials and Methods

2.1 Material preparation

Q235 carbon steel was used for the measurements and the chemical composition of the specimens was listed in Table 1. The specimens were cut out from a cold rolled sheet of 2 mm thick before measurements and coated with High-temp RTV silicone gasket to keep the exposed surface 15 mm × 15 mm. The specimens had been abraded gradually from 180 to 1000 grit silicon carbide paper. Then they were rinsed with deionized water and acetone, dried and stored before use.

Table 1. Chemical composition of Q235 carbon steel.

C	Mn	Si	S	P
≤0.22%	0.3% - 0.65%	≤0.35%	≤0.05%	≤0.045%

2.2 Corrosion conditions

The corrosion solution consisted of 2000 mg/L $NaHCO_3$ in the presence of different concentration of NaCl, ranging from 500 mg/L to 1200 mg/L. The pH value and temperature used in the corrosion experiments were 6.7 and 25 ℃, respectively.

2.3 Setup of acoustic emission monitoring

The AE acquisition system and pitting assembly are shown in Figure 1. The AE acquisition system was consisted of Mistras USB AE Node, sensor R15α (50 - 200K Hz). The sensor was assembled by spring applying 6 N forces. The high vacuum grease was used between interface of sensor and specimen to ensure the best connection. The AE acquisition options are shown in Table 2.

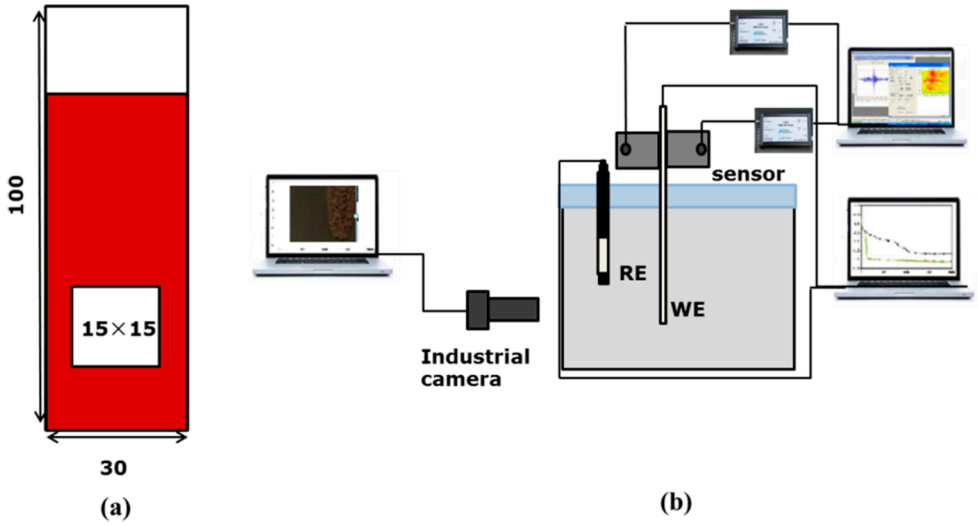

Figure 1. The schematic diagram of AE monitoring pitting corrosion: (a) Q235 specimen (dimension in mm), (b) pitting assembly and the AE system and potential measurement.

Table 2. AE acquisition options.

Threshold	PDT	HDT	HLT	Analog filter	Sample rate	Pre-Trigger	Length
27dB	200μs	400μs	200μs	100K-400KHz	2MPS	40μs	2K

2.4 Electrochemical measurements and corrosion morphologies observation

Open circuit potential (OCP) was measured by a CHI4 electrochemical workstation of Wuhan Corrtest Instruments Corp. LTD in China. Specimens of Q235 carbon steel were used as work electrodes. A saturated calomel electrode (SCE) was used as the reference electrode. The corrosion morphologies were recorded by industrial digital camera (Yilong Electronic Technology Co. Ltd, Shenzhen, China, 5 mega-pixel) during experiment and scanning electron microscope (SEM, ZEISS, EVO, MA 15) after the experiments. The OCP and AE measurements were carried out and recorded simultaneously.

3. Results

3.1 AE and OCP monitoring

Figure 2 shows the OCP and AE monitoring of corrosion process of Q235 carbon steel in 2000 mg/L $NaHCO_3$ in the presence of different concentrations of NaCl. In Figure 2a, OCP behaved differently with time in various NaCl concentrations. It slightly moved to the positive direction and gradually stabilized after 50000 seconds' immersion in the presence of 500 mg/L NaCl, indicating the interface condition was relatively and lightly influenced by the presence of NaCl. With the increase of NaCl concentration, the OCP behavior changed. In 800 mg/L NaCl, OCP shifted negatively and could not reach the stable state in nearly 90000 s immersion time. In the NaCl concentration of 1000 mg/L NaCl and 1200 mg/L, OCP moved sharply towards negative direction and reached a relative stable state at 65000 s and 30000 s, respectively. The above results revealed the different interface conditions of carbon steel in $NaHCO_3$ solution in the presence of different concentrations of NaCl. It was commonly believed that the iron oxide and ferrous bicarbonate can be formed as passive film of carbon steel in bicarbonate solutions [5-6]. The addition of chloride iron accelerated the breakdown of the passive film and triggered the initiation of pitting. The higher concentration of Cl^-, the faster the passive film broken and the OCP stabilized.

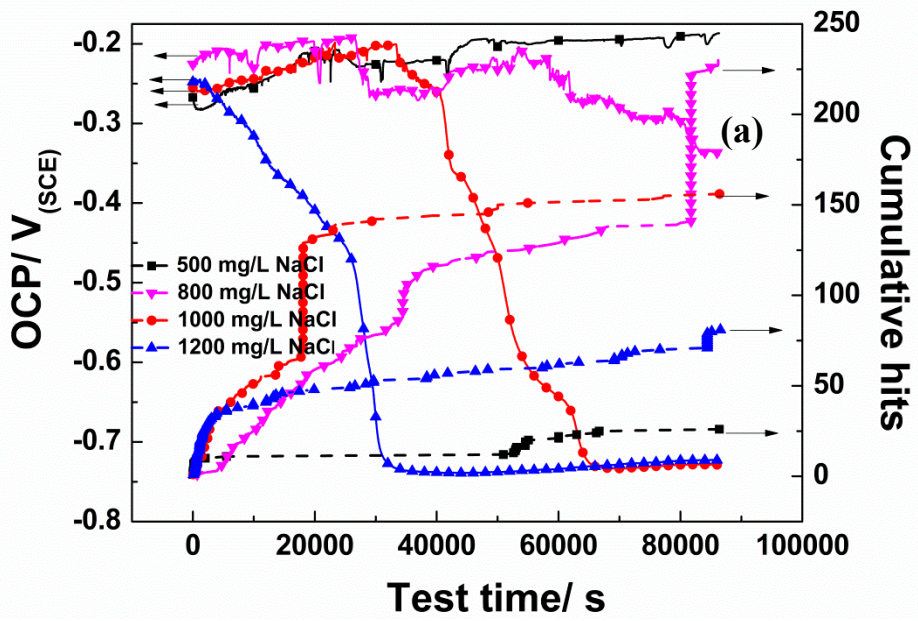

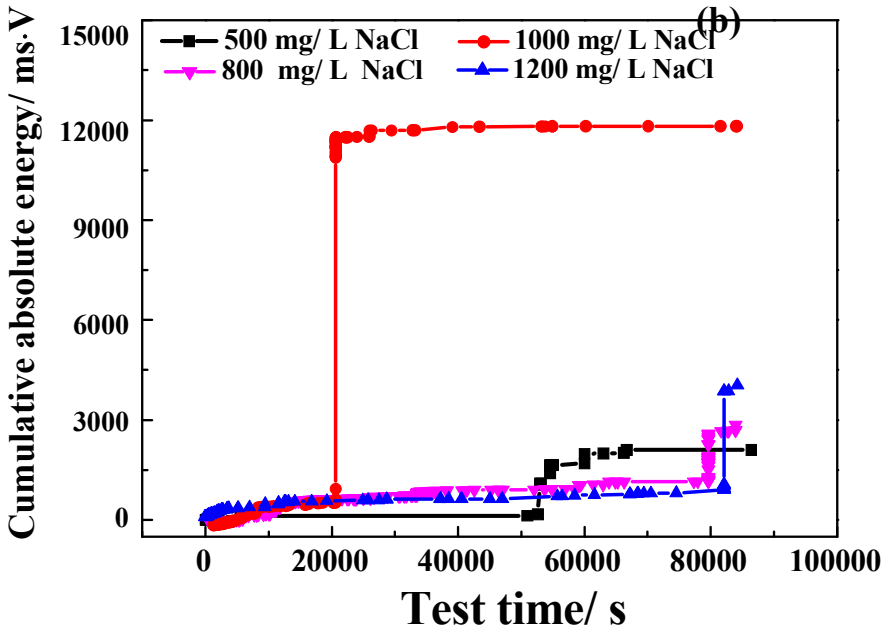

Figure 2. The OCP and AE monitoring of pitting corrosion of carbon steel in NaCl + $NaHCO_3$ solutions: (a) OCP and cumulative hits versus time, (b) cumulative absolute energy versus time.

Figure 2a also presented the influence of NaCl concentration on cumulative hits of acoustic emission and the correlation between OCP and cumulative hits. In concentration of 500 mg/L, the cumulative hits kept at very low level at the first 5000 s then started to increase slightly, indicating the corrosion events happened in such Cl^- concentration were not very noticeable. The few cumulative hits in AE monitoring is in accord with the relative small variation range of OCP.

Cumulative hits continuously increased with time in the presence of 2000 mg/L $NaHCO_3$ + 800 mg/L NaCl, which represented the happening of corrosion events all the time. The repeating of metal dissolution beneath the cover of pits (occluded cell) and the initiation of new pits resulted in the continuous [6] increasing of cumulative hits. Probably the breakdown of corrosion product film upon the occlude cell induced the sudden ascending of cumulative hits at about 80000 s because this process could be high emissive of acoustic emission.

The cumulative hits behaved differently in 1000 mg/L and 1200 mg/L of NaCl. In 1000 mg/L NaCl solution, cumulative hits increased quickly with time and suddenly vised at about 20000 s, indicating breakdown of passive film in localized area. Then the cumulative hits increased slowly with time. However, in 1200 mg/L NaCl, the cumulative hits increased very fast at the beginning then gradually and slowly with time, indicating a relative stable development of corrosion attack on the surface after 5000 s. Before that time, the pitting corrosion started from the first second and propagated very fast. In another hand, the OCP stabilized (even a slightly increasing trend) at a certain time in 1000 mg/L (65000 s) and 1200 mg/L (30000 s), which indicated the stage of stable propagation. The high emissive period of AE was before this stage in these two solutions. The results of AE monitoring and OCP monitoring were in agreement. It was noticed that the significant increasing in AE hits was earlier than the sharply drop of OCP in these two experiments. It revealed that the AE monitoring is more sensitive to the corrosion evolution compared with OCP monitoring.

It is interesting that the cumulative hits still kept increasing after the stabilization of OCP curve. The nature of pitting corrosion is a random sporadic and stochastic [37]. Therefore, the initiation, accelerated propagation, stable growth/ repassivation of pitting corrosion are hard to be predicted. In most circumstances, pitting corrosion happens and propagates at some localized sites independently. The OCP behavior represents the general thermodynamic property of the whole interface, which depends on the pitting is whether meatastable or stable, in which stage - initiation, accelerated propagation, stable growth or repassivation and even the number of active pits. While the increase of cumulative hits stands for the new corrosion events at any local area. These corrosion events refer to any event during corrosion initiation, propagation and stable growth. While for the whole interface, such corrosion events may have no apparent influence on OCP in stable growth stage. However, only the AE signal amplitude of these events exceed the threshold of AE acquisition setup, the record of AE data can be trigged. That is, the cumulative AE hits in Figure 2 only increased for such corrosion events which can generate AE signal with the amplitude equal or higher than 27 db.

Figure 2b shows the cumulative absolute energy changes over time of AE monitoring. Basically, the higher AE hits activity, the faster increase of absolute energy than other stages in the experiments as shown in Figure 2b except in 1200 mg/L NaCl solution. The acoustic emission of corrosion event not only depended on the corrosion stages and also corrosion morphology and other factors such as the propagation route of pits (i.e. go through the crystalline grain or boundary), so did the energy of AE. Although the energetic AE signals in pitting is normally corresponding to the propagation [23, 24] and hydrogen bubble burst, the formation and peeling of thick corrosion products also may generate energetic AE signals if they existed in 1200 mg/L NaCl solution.

3.2 Surface morphology monitoring of pitting corrosion

Figure 3 shows the surface morphologies from in-situ monitoring of the propagation of pitting corrosion in different Cl^- concentrations at different time intervals, 0 s, 40000 s, 60000 s and 80000 s, respectively. The surface morphology monitoring experiments were conducted simultaneously with the OCP and AE measurements. After the experiments, the surface morphologies of pits after removing loosened corrosion products were observed by SEM, as shown in Figure 4.

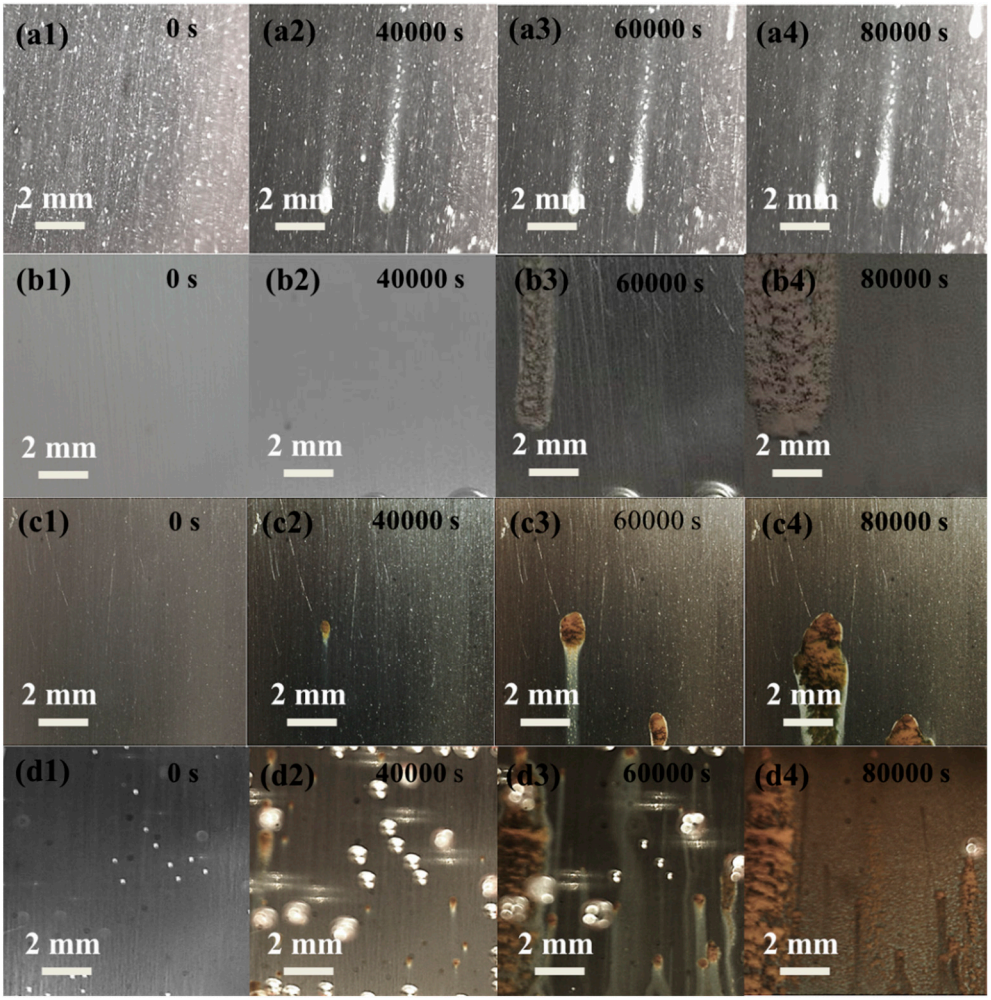

Figure 3. Surface morphologies from in-situ monitoring the propagation of pitting corrosion of carbon steel with optical microscope in the solutions with different concentrations of chloride ion: (a1), (a2), (a3), (a4) 500 mg/L NaCl, (b1), (b2), (b3), (b4) 800 mg/L NaCl, (c1), (c2), (c3), (c4) 1000 mg/L NaCl, (d1), (d2), (d3), (d4) 1200 mg/L NaCl.

In the presence of 500 mg/L NaCl, several pits can be observed on the surface after 40000 s' immersion. It can be seen from the images that the pits had not grown apparently with immersion time prolonged, indicating the pits had re-passivated and would not propagated to any more. SEM images also proved, Figure 4 (a) and (b), that the pits were open and shallow, without the cover of corrosion products. This type of pitting emitted weak AE signals because it was caused by localized anodic dissolution which is not an effective generation source of AE. And some of them may be too weak to pass the threshold of 27 dB in acquisition setup.

No apparent pits can be observed on carbon steel surface by optical microscope before 40000 s in the presence of 800 mg/L NaCl. But the occluded cell had been formed on the specimen surface. This was the reason of the increase of cumulative hits at the experiments beginning. After 40000 s, two pits gradually initiated and propagated on the surface. The pits kept growing with immersion time and the corrosion damage area in 80000 s became rather big. This behavior was in accordance with the variation of cumulative hits very well. In addition, many corrosion products can be observed on the damage area. Occluded environment beneath corrosion products had been formed, which accelerated the propagation of the pitting corrosion. SEM images showed some corrosion products covered on the pit, shown in Figure 4c and 4d. The carbon steel beneath the cover would keep dissolving in the occluded area, which corresponded to the continuous rising of cumulative hits in Figure 2.

Peer-reviewed version available at Appl. Sci. 2019, 9, 706; doi:10.3390/app9040706

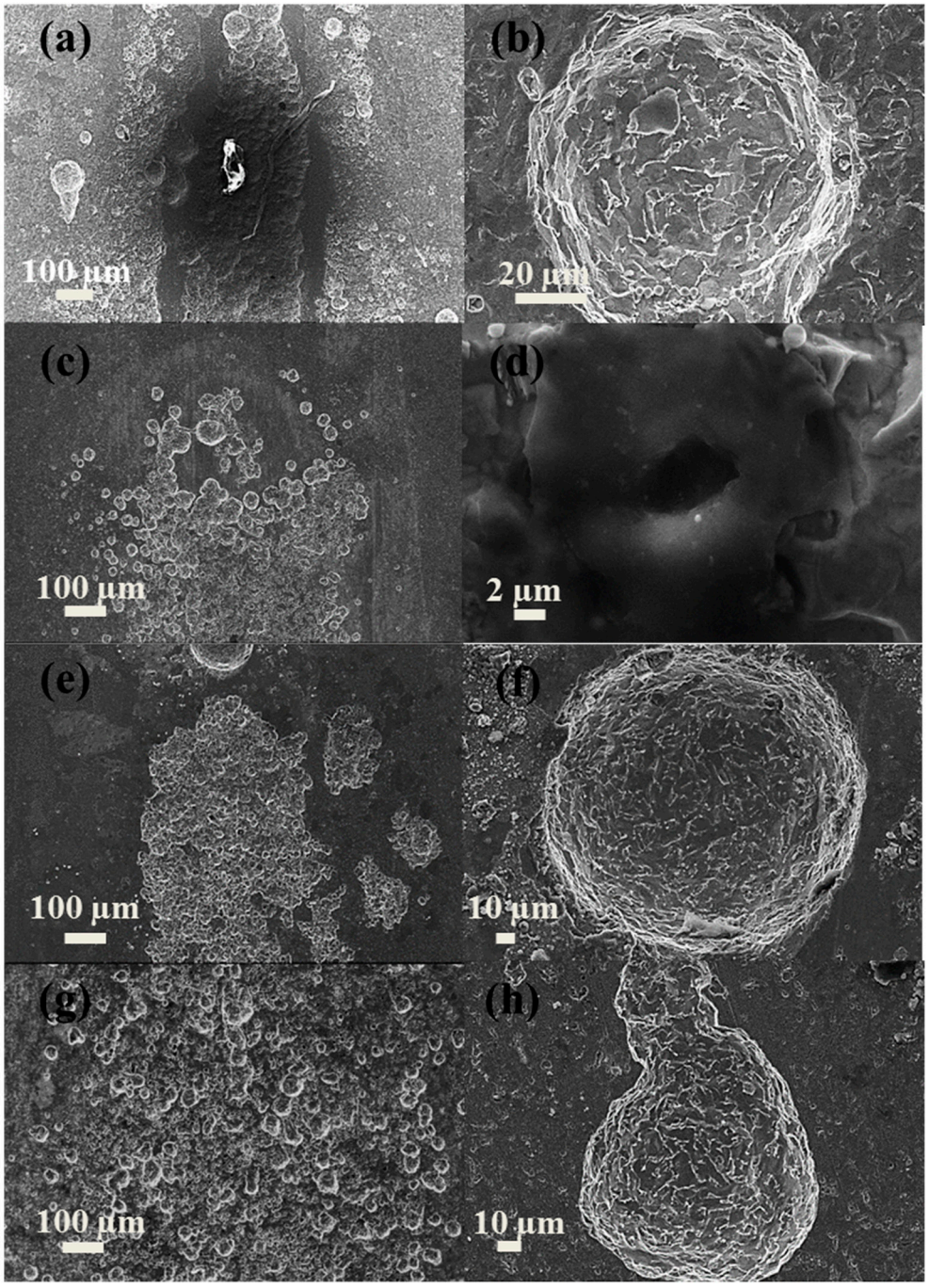

Figure 4. SEM morphologies of Q235 carbon steel after immersion for 86400 s in 2000 mg/L $NaHCO_3$ and NaCl concentration of: (a) and (b) 500 mg/L NaCl, (c) and (d) 800 mg/L NaCl, (e) and (f) 1000 mg/L NaCl, (g) and (h) 1200 mg/L NaCl, loosened corrosion products were removed.

The corrosion morphology evolution and SEM images of specimen in 1000 mg/L neutral NaCl solution are shown in Figure 3c1-c4 and Figure 4e-f. Two apparent pits can be observed on the specimen surface at 40000 s, which kept growing with immersion time. Many corrosion products can be observed on the damage area at 80000 s. The SEM images showed that there were some shallow and small pits on the sample surface. However, because the solution became more corrosive, the corrosion started earlier and its rate became higher. As a result, higher AE activity was recorded in the beginning time of monitoring and the AE hits in a short duration near 20000 s showed high absolute energy.

As implied by OCP, the sample of Q235 carbon steel was corroded as soon as it was put in 1200 mg/L NaCl solution, as shown in Figure 3d1-d4, combined with the cumulative hits curve in Figure

2, corrosion initiation and propagation were very fast from the first second. Correspondingly, there were highest AE activities in the beginning period but without high energy. This can be attributed to the shallow and open shapes of pits, as shown in Figure 4g-h. The corrosion mechanism of carbon steel belongs to general corrosion at high Cl^- concentration while pitting corrosion at low Cl^- concentration. Thus in the $NaHCO_3$ solution with 1200 mg/L NaCl, the localized corrosion tendency has been weakened. Finally, most surface of the test sample were covered by corrosion products as shown in Figure 3d4. Nevertheless, the coverage of corrosion products on the carbon steel surface non-uniformly will enhance the occluded effect, which could promote the localized corrosion and the AE generation.

3.3 Waveform processing

The acoustic signals from experiments were recorded by AE system. Figure 5a shows a typical waveform of acoustic signal of carbon steel in $NaHCO_3$ + NaCl solution. It is shown that some information of the waveform, the beginning and end of which, was not useful. So, additional processing of the signals is necessary for the preparation of further analysis. Herein, three steps, including pre-trigger removing, Tail-cutting and shape preserving interpolation (SPI), had been applied to process the waveform in Matlab. Pre-trigger removing, a value tells the software how long to record (in μsec) before the trigger point (the point at which the threshold is exceeded), aimed at removing digital noise from acquisition. Tail-cutting was used to remove the "zero-padding" which may have been applied at the end on some waveforms during the acquisition process (Figure 5b). SPI was an effective tool to keep each waveform has a same number of points to be stored which based on the Piecewise Cubic Hermite Interpolating Polynomial (PCHIP) technique and the Weierstrass Approximation Theorem. The waveform after processing is shown in Figure 6. In this study, wavelet denoising was performed by the Matlab wavelet tool box (Figure 7). The treated waveform by denoising had been stored for processing and extracting parameters.

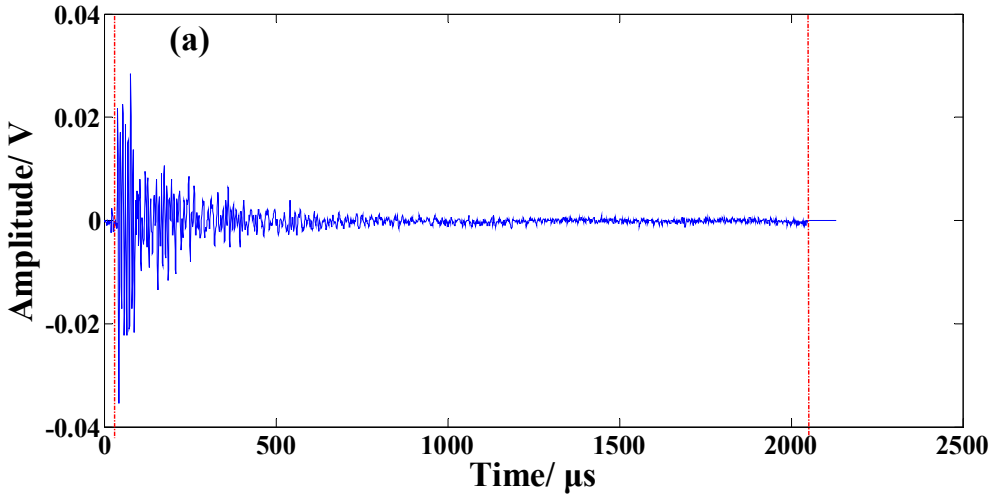

Peer-reviewed version available at Appl. Sci. 2019, 9, 706; doi:10.3390/app9040706

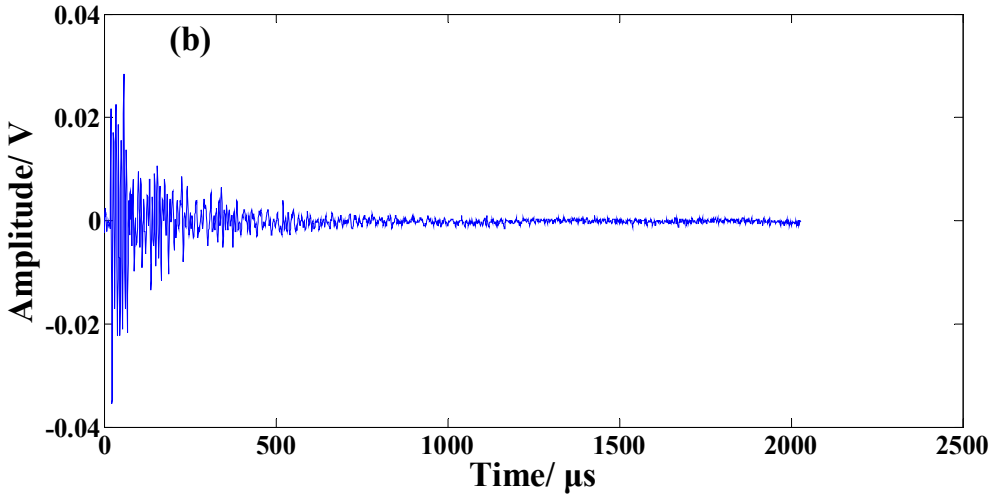

285

286 **Figure 5.** The Waveform processing of a typical acoustic signal obtained from Q235 carbon steel in
287 $NaHCO_3$ + NaCl solution: (a) original, (b) pre-trigger removed and tail cut.

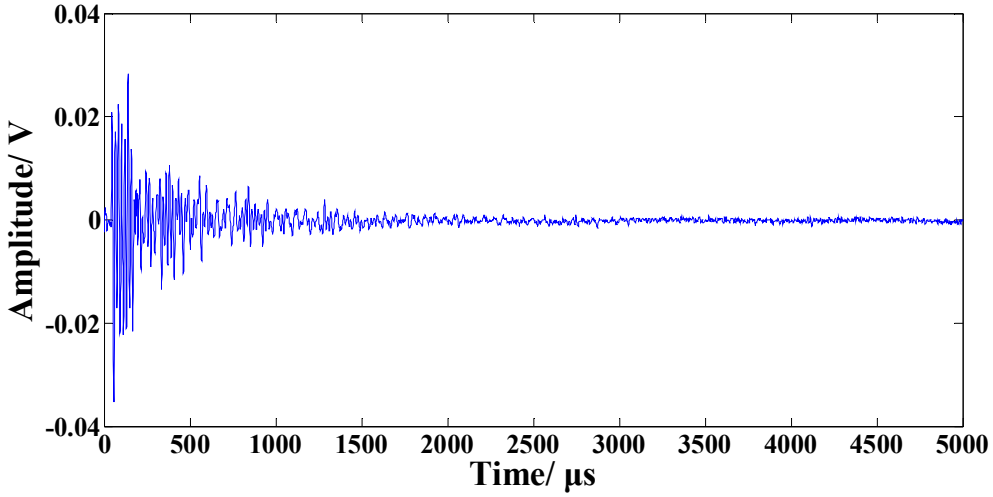

288

289 **Figure 6.** The processed waveform of a typical acoustic signal obtained from Q235 carbon steel in
290 $NaHCO_3$ + NaCl solution (after SPI and wavelet denoised).

Peer-reviewed version available at Appl. Sci. 2019, 9, 706; doi:10.3390/app9040706

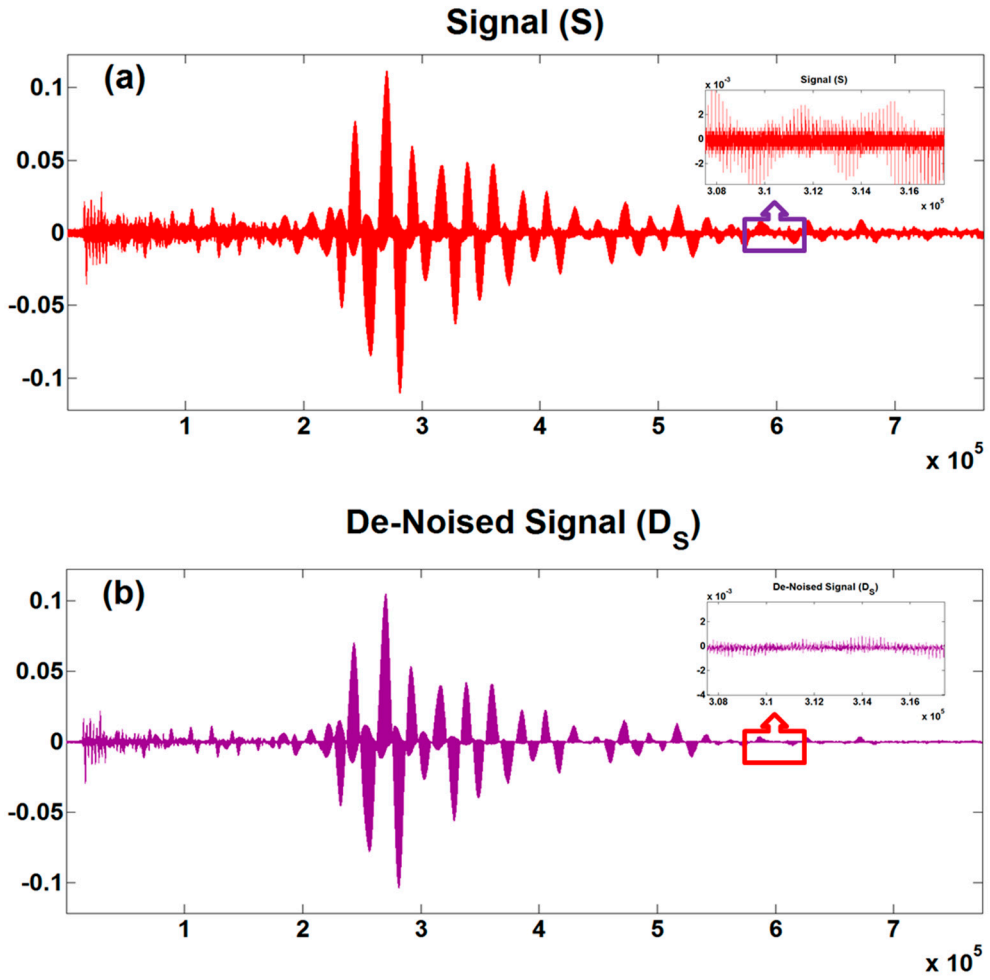

Figure 7. Denoising method for a typical signal of acoustic emission of carbon steel in $NaHCO_3$ + NaCl solution. (a) signal before denoising, (b) signal after denoising.

3.4 Clustering analysis

A function was established to input waveform information, time and system information contain maximum duration, hit definition time (HDT), hit lockout time (HLT), peek definition time (PDT), sampling frequency, threshold to Matlab.

After extracting feature, these new parameters were plotted in different correlation diagrams. The comparison between original parameters and new parameters under different corrosion conditions are shown in Figure 8 and Figure 9. These results showed that the performing of signal processing as developed can effectively classify AE signals in the correlation diagram.

Peer-reviewed version available at Appl. Sci. 2019, 9, 706; doi:10.3390/app9040706

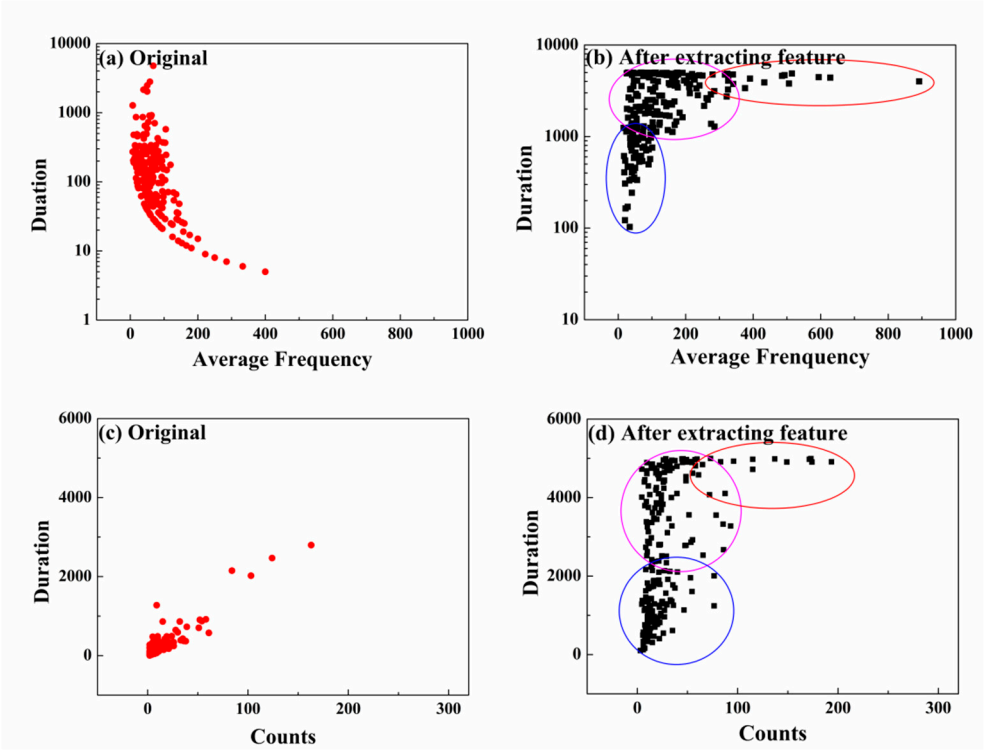

Figure 8. Parameters analyzing of signals of Q235 carbon steel in 2000 mg/L $NaHCO_3$ + 800mg/L NaCl: (a) and (c) original relationship of duration-average frequency and duration-counts, (b) and (d) relationship of duration-average frequency and duration-counts after extracting feature.

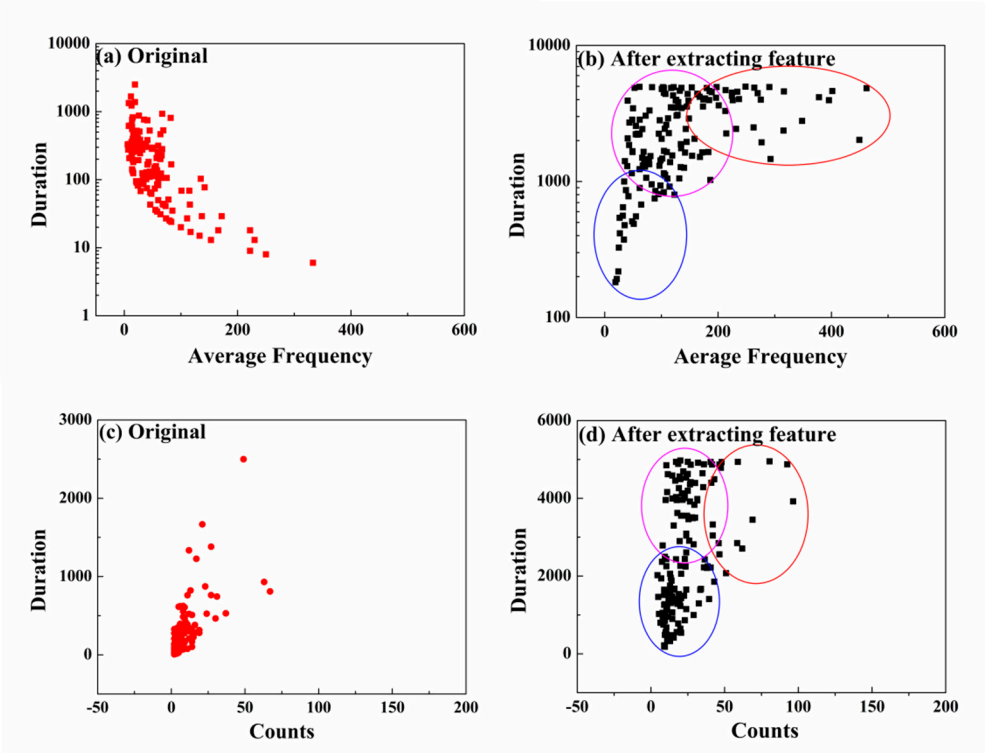

Figure 9. Parameters analyzing of signals of Q235 carbon steel in 2000 mg/L $NaHCO_3$ + 1000mg/L NaCl: (a) and (c) original relationship of duration-average frequency and duration-counts, (b) and (d) relationship of duration-average frequency and duration-counts after extracting feature.

Based on the analyzing of the relationship between duration and average frequency of AE waveforms，the AE signals of Q235 carbon steel in different corrosive media (2000 mg/L $NaHCO_3$ + 800 mg/L NaCl and 2000 mg/L $NaHCO_3$ + 1000 mg/L NaCl solution) during pitting process could be classified into three types: high duration with high frequency, high duration with low frequency and low duration with low frequency. In addition, the three groups of signals can be identified according to the duration versus counts correlation diagram: low duration with low counts, high duration with low counts and high duration with high counts.

The representative waveforms of the three type signals are shown in the Figure 10. The low duration with low frequency and low counts signals appeared most frequently in the beginning of the experiment. They were burst signal (Figure 10a) or asymmetric signal (Figure 10b), indicating that they should belong to the corrosion event of surface breakdown. Most of the high duration with low frequency and low counts signals occurred during the accelerating propagation of pitting corrosion. They were resonant signals (Figure 10c). In the stable growth process of pitting corrosion after accelerated propagation, the AE waveforms were also resonant signals. But the signal feature was more complex than that in the accelerated propagation process (Figure 10d), which may be due to the combination of the breakdown of corrosion products and the growth of the pits at the same time. Above result is consistent with other studies on the acoustic emission of the pitting corrosion [23, 35-36].

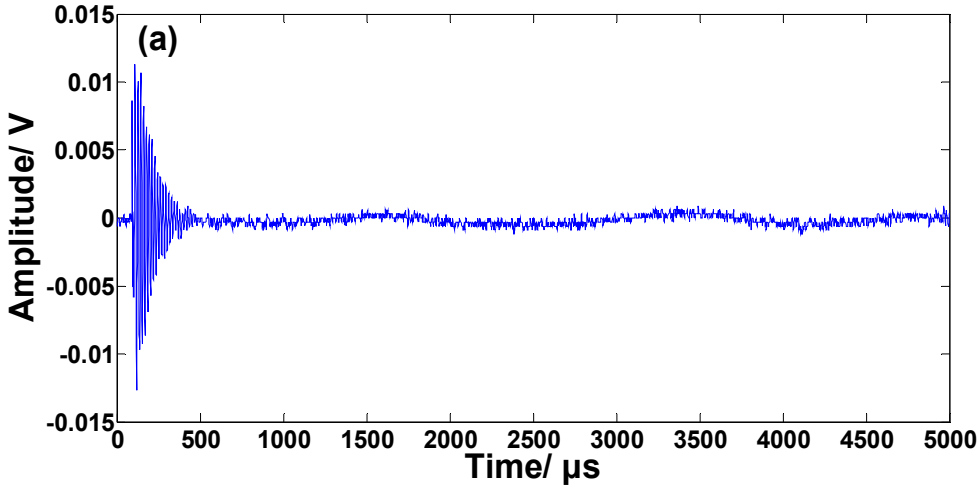

3.5 Cor

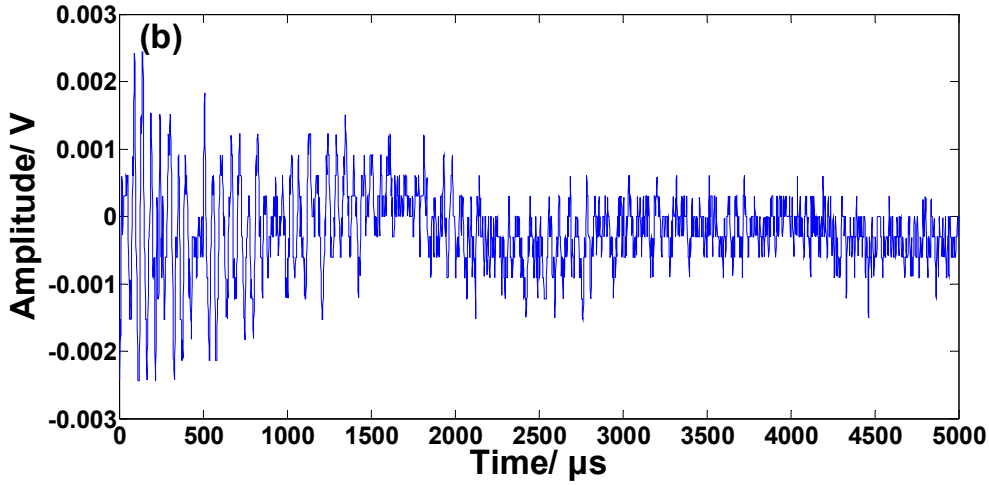

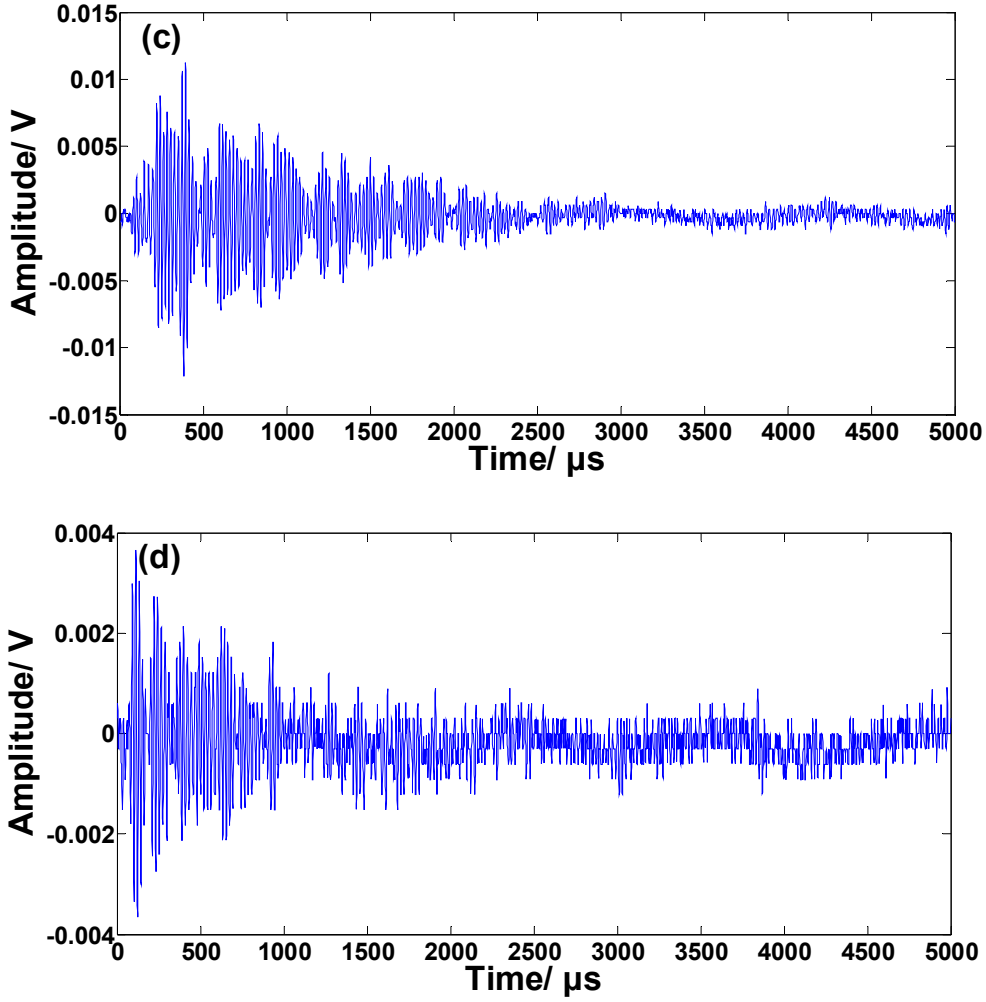

Figure 10. Waveforms from top to bottom: (a) and (b) low duration with low frequency and low counts, (c) high duration with low frequency and low counts, (d) high duration with high frequency and high counts.

3.5 Corrosion type identification

In order to identify the different corrosion types in the corrosion process fast and effectively, a 2D pattern recognition algorithm was established by Matlab. This processing algorithm provides a new feasible method for the identification of different acoustic emission data directly from the waveform of AE signal without the extraction of AE parameters.

In 2D pattern recognition analysis, the luminance information of the object surface is related to the illumination and reflection coefficient. Otherwise, the structure and illumination of the objects in the scene are independent. The reflection coefficient and the related objects are the same. We can explore the structure information in an image by separating the illumination effect of objects. Here, the object and structure relate to the brightness and contrast as the structure information of the image definition. Because the brightness and contrast of a scene are always changing, we can do local processing to get more accurate results.

The measurement of similarity is composed of three modules: luminance, contrast ratio, structure. Their functions are defined as follows:

First of all, for the discrete signal, we use the average gray level as a measure of the intensity of the estimation as function (1) shows, and the brightness contrast function $\angle(x, y)$ is a function about μ_x and μ_y.

$$\mu_x = (1/N)\sum_{1}^{N} x_i \quad (1)$$

Preprints (www.preprints.org) | NOT PEER-REVIEWED | Posted: 6 November 2018 doi:10.20944/preprints201811.0131.v1

Peer-reviewed version available at Appl. Sci. 2019, 9, 706; doi:10.3390/app9040706

Then, the average gray value should be removed from the signal based on the measurement system. For the discrete signal x – μ_x, the standard deviation can be used to do the contrast measure such as function (2) shows, and the contrast function $c(x,y)$ of contrast is a function of σ_x and σ_y.

$$\sigma_x = \left(1/N - 1 \sum_{i=1}^{N} (x_i - \mu_x)^2 \right)^{1/2} \quad (2)$$

Next, the signal is divided by their standard deviation, contrast function structure is defined as a function of $\frac{(x-\mu_x)}{\sigma_x}$ and $\frac{(y-\mu_y)}{\sigma_y}$.

Finally, the three contrast modules are combined into a complete similarity measure function:

$$S(x,y) = \big(l(x,y), c(x,y), s(x,y)\big) \quad (3)$$

S (x, y) should meet the following three conditions:

Symmetry: $S(x,y) = S(y,x)$,

Bounded property: $S(x,y) \leq 1$,

Maximum uniqueness: $S(x,y) = 1$, when and only when $x = y$.

Then, the three contrast functions are defined, and finally they are combined to get the following similarity function:

$$SSIM(x,y) = [l(x,y)]^{\alpha}[c(x,y)]^{\beta}[s(x,y)]^{\gamma} \quad (4)$$

When $\alpha = \beta = \gamma = 1$, a function would be got as follows:

$$SSIM(x,y) = \big(2\mu_x\mu_y + C_1\big)\big(2\sigma_x\sigma_y + C_2\big)/\big(\mu_x^2 + \mu_y^2 + C_1\big)\big(\sigma_x^2 + \sigma_y^2 + C_2\big) \quad (5)$$

Other corrosion types were monitored by AE aiming at calculating similarities among them. Pitting corrosion of stainless steel in the presence of different concentrations of chloride ions and uniform corrosion of carbon steel in sulphuric acid solution were monitored by the same device as Figure 1. The specimens of crevice corrosion of stainless steel were pretreated based on ASTM G39-1999(2011) and monitored by the method of Y. Kim [38], and AE waveforms of different types of corrosion were arranged in time sequence. Figure 11 shows the continuous AE waveform graphics and the similarity calculation results between them are exhibited in Table 3.

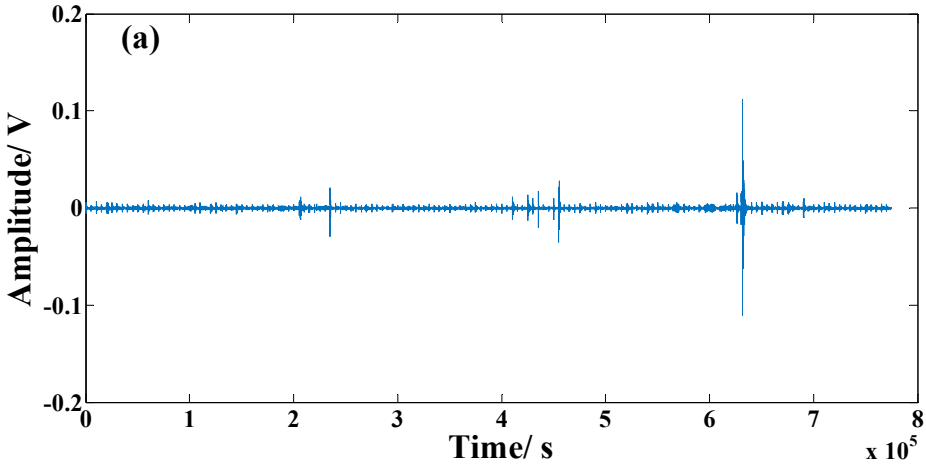

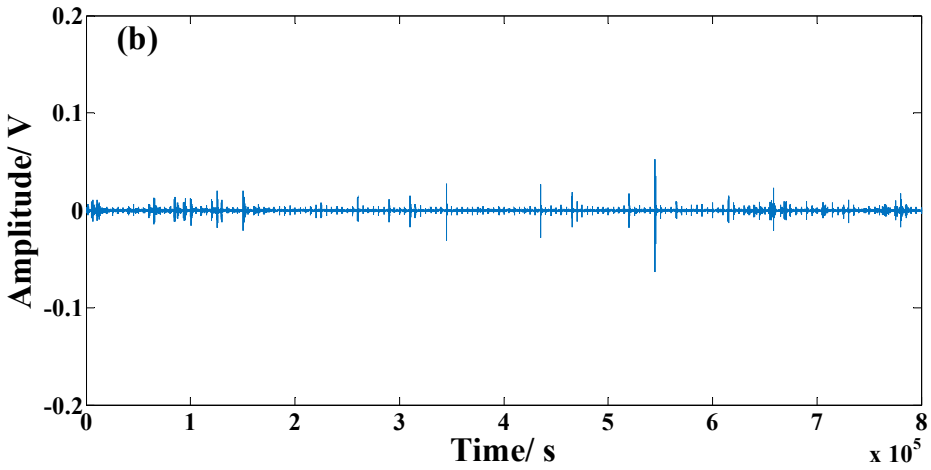

373

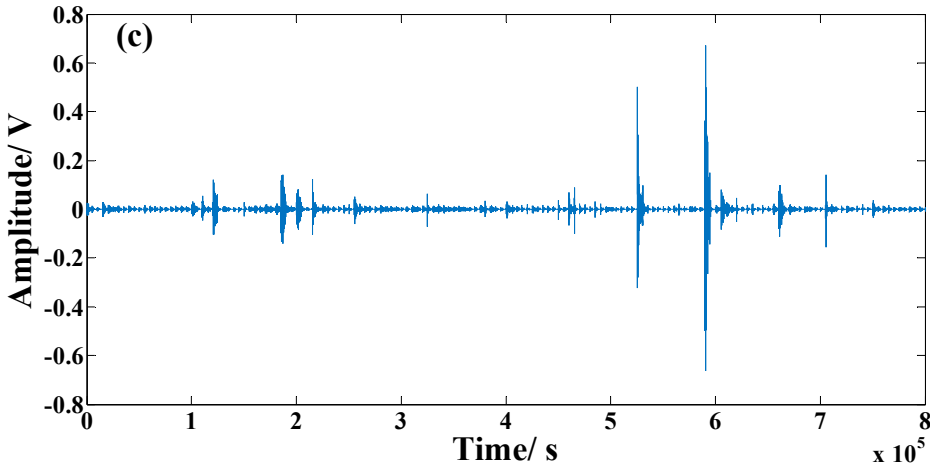

374

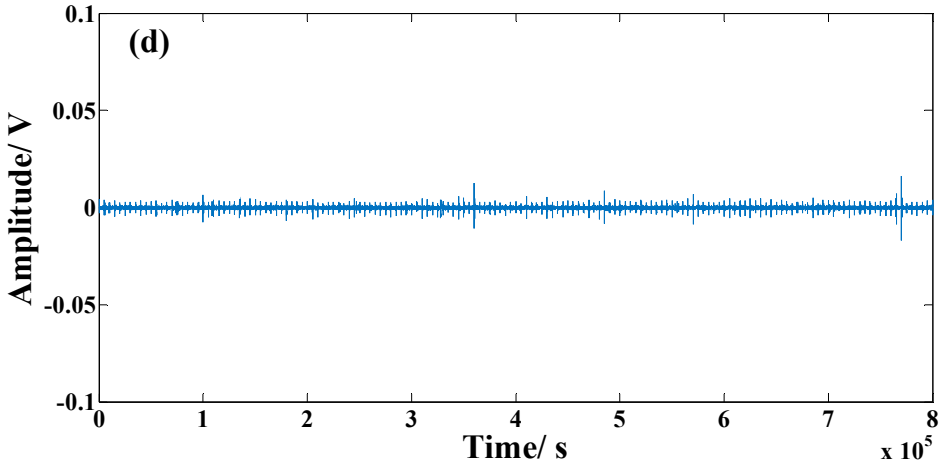

375

Peer-reviewed version available at Appl. Sci. 2019, 9, 706; doi:10.3390/app9040706

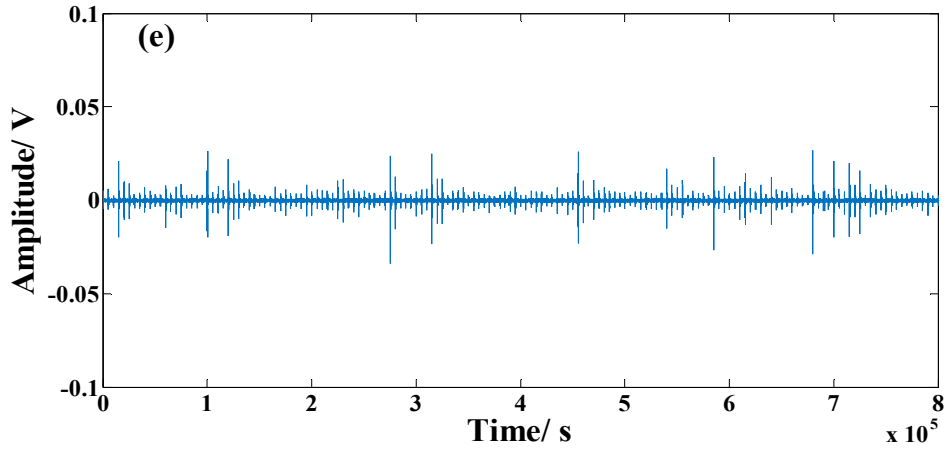

Figure 11. Different continuous AE graphics: (a) pitting corrosion of carbon steel, (b) pitting corrosion of stainless steel, (c) crevice corrosion of stainless steel, (d) uniform corrosion of carbon steel, (e) noise.

Table 3. The similarity of different types of corrosion

	Pitting corrosion Carbon steel	Crevice corrosion Stainless steel	Uniform corrosion Carbon steel	Noise
Pitting corrosion Stainless steel	83.23	78.03	50.12	27.53
Pitting corrosion Carbon steel		85.51	52.16	48.74
Crevice corrosion Stainless steel			35.41	45.13
Uniform corrosion Carbon steel				42.13

According to the calculation results, there was a high similarity between pitting corrosion of carbon steel and that of stainless steel. The occluded cell of the pitting corrosion on carbon steel was not stable in performed experiments. The repeating of occluded cell formation and rupture process caused the open pits on the surface of carbon steel. In contrast, the pitting corrosion of stainless steel had a relatively strong occlusion effect. So that the corrosion pit of stainless steel often had small mouth with relative bigger depth. However, in essence, these two kinds of pitting corrosion were all caused by the occlusion effect, from which they had the similar acoustic emission process (83.23% similarity) as shown in Table 3. In addition, the corrosion process of the 2D images of pitting corrosion and crevice corrosion also had a high degree of similarity (73.03%), which is related to their corrosion mechanisms are relatively similar [34]. On the other hand, the graphic of uniform corrosion has a low similarity with other types of corrosion, indicating that this data processing approach is able to

identify localized corrosion from uniform corrosion. In addition, the AE graphic of artificial made noise from solution stirring also has low similarities with all corrosion graphics.

4. Conclusions

The pitting corrosion of Q235 carbon steel in $NaHCO_3$ + NaCl solutions was studied by in-situ monitoring of the AE technique and OCP simultaneously. The concentration of NaCl had pronounced influence on OCP evolution. In 500mg/L NaCl, OCP varied in a very narrow range, indicating a relative stable state. However, with the increase of NaCl concentration, OCP dropped significantly and stabilized at the rather negative potential.

The AE monitoring results were in accordance with the results of OCP monitoring. However, OCP only presented the thermodynamic information of corrosion in the interface, while AE sensor can detect the breakdown of passive film, small damage in occluded pits under metallic surface and relative events.

AE signals of pitting corrosion on carbon steel can be classified into three types by waveform parameters clustering after AE waveform processing, including pre-treatment, shape preserving interpolation and denoising. The result indicated that the signal processing as developed is a highly efficient method for classifying AE signals and preparing waveform for further data analysis.

The method based on 2D pattern recognition had been established for identifying different types of corrosion in Matlab. The analysis results showed that the method can be used to distinguish the uniform corrosion and localized corrosion effectively, while it is not very effective to distinguish the different localized corrosion.

Author Contributions: Conceptualization, J. T. and H. W.; methodology, J. T. and H. W.; software, J. T. and H. W.; investigation, J. T., H. W. and G. C.; data curation, J. L.; writing—original draft preparation, J. T. and Y. W.; writing—review and editing, J. T. and Y. W.; visualization, J. T. and J. L.; supervision, H. W.

Funding: This research was funded by Applied Basic Research Programs of Science and Technology Department of Sichuan Province, grant number 2017JY0044 and Project Funding to Scientific Research Innovation Team of Universities Affiliated to Sichuan Province, grant number 18TD0012.

Conflicts of Interest: The authors declare no conflict of interest.

References

1. Tsangouri, E.; Karaiskos, G.; Deraemaeker, A.; Hemelrijck, D. Van Assessment of Acoustic Emission localization accuracy on damaged and healed concrete. Constr. Build. Mater. 2016, 129, 163–171, doi:10.1016/j.conbuildmat.2016.10.104.
2. Parks, J.E.; Papulak, T.; Pantelides, C.P. Acoustic emission monitoring of grouted splice sleeve connectors and reinforced precast concrete bridge assemblies. Constr. Build. Mater. 2016, 122, 537–547, doi:10.1016/j.conbuildmat.2016.06.076.
3. Zaki, A.; Kian, H.; Behnia, A.; Aggelis, D.G.; Ying, J.; Ibrahim, Z. Monitoring fracture of steel corroded reinforced concrete members under flexure by acoustic emission technique. Constr. Build. Mater. 2016, doi:10.1016/j.conbuildmat.2016.11.079.
4. Bardal, E. Corrosion and Protection; Springer London, 2004;
5. Tang, Y.M.; Zuo, Y.; Zhao, X.H. The metastable pitting behaviors of mild steel in bicarbonate and nitrite solutions containing Cl À. 2008, 50, 989–994, doi:10.1016/j.corsci.2007.12.003.
6. Li, W.S.; Luo, J.L. Uniformity of passive films formed on ferrite and martensite by different inorganic inhibitors. 2002, 44, 1695–1712.
7. Eduardo, C.; Souza, D.A.; Gonçalves, C.; Costa, F.; Petronilha, A.; Reis, M.; Castro, D.; Freitas, V. De; Lins, C. Corrosion failure analysis in a biodiesel plant using electrical resistance probes. EFA 2016, 66, 365–372, doi:10.1016/j.engfailanal.2016.05.018.
8. Legat, A. Monitoring of steel corrosion in concrete by electrode arrays and electrical resistance probes. 2007, 52, 7590–7598, doi:10.1016/j.electacta.2007.06.060.
9. Civil, A.O.F. New non-destructive method for linear polarisation resistance corrosion rate measurement. 2010, X, doi:10.1016/S1644-9665(12)60053-3.

10. Gan, F.; Wan, Z.; Li, Y.; Liao, J.; Li, W. Improved formula for localized corrosion using field signature method. 2015, 63, 137–142, doi:10.1016/j.measurement.2014.12.008.
11. Hass, F.; Abrantes, A.C.T.G.; Diógenes, A.N.; Ponte, H.A. Evaluation of naphthenic acidity number and temperature on the corrosion behavior of stainless steels by using Electrochemical Noise technique. Electrochim. Acta 2014, 124, 206–210, doi:10.1016/j.electacta.2013.08.090.
12. Rubio, M.A.; Bethune, K.; Urquia, A.; St-Pierre, J. Proton exchange membrane fuel cell failure mode early diagnosis with wavelet analysis of electrochemical noise. Int. J. Hydrogen Energy 2016, 41, 14991–15001, doi:10.1016/j.ijhydene.2016.05.292.
13. Tang, J.; Soua, S.; Mares, C.; Gan, T.H. An experimental study of acoustic emission methodology for in service condition monitoring of wind turbine blades. Renew. Energy 2016, 99, 170–179, doi:10.1016/j.renene.2016.06.048.
14. Tranchot, A.; Etiemble, A.; Thivel, P.X.; Idrissi, H.; Roué, L. In-situ acoustic emission study of Si-based electrodes for Li-ion batteries. J. Power Sources 2015, 279, 259–266, doi:10.1016/j.jpowsour.2014.12.126.
15. Datt, P.; Kapil, J.C.; Kumar, A. Acoustic emission characteristics and b-value estimate in relation to waveform analysis for damage response of snow. Cold Reg. Sci. Technol. 2015, 119, 170–182, doi:10.1016/j.coldregions.2015.08.005.
16. Gagar, D.; Foote, P.; Irving, P.E. Effects of loading and sample geometry on acoustic emission generation during fatigue crack growth: Implications for structural health monitoring. Int. J. Fatigue 2015, 81, 117–127, doi:10.1016/j.ijfatigue.2015.07.024.
17. Merson, E.; Vinogradov, A.; Merson, D.L. Application of acoustic emission method for investigation of hydrogen embrittlement mechanism in the low-carbon steel. J. Alloys Compd. 2015, 645, S460–S463, doi:10.1016/j.jallcom.2014.12.083.
18. Kim, Y.P.; Fregonese, M.; Mazille, H.; Féron, D.; Santarini, G. Ability of acoustic emission technique for detection and monitoring of crevice corrosion on 304L austenitic stainless steel. NDT E Int. 2003, 36, 553–562, doi:10.1016/S0963-8695(03)00065-3.
19. Teófilo, E.T.; Rabello, M.S. The use of acoustic emission technique in the failure analysis of PET by stress cracking. Polym. Test. 2015, 45, 68–75, doi:10.1016/j.polymertesting.2015.05.005.
20. Hwang, W.; Bae, S.; Kim, J.; Kang, S.; Kwag, N.; Lee, B. Acoustic emission characteristics of stress corrosion cracks in a type 304 stainless steel tube. Nucl. Eng. Technol. 2015, 47, 454–460, doi:10.1016/j.net.2015.04.001.
21. Ferrer, F.; Idrissi, H.; Mazille, H.; Fleischmann, P.; Labeeuw, P. Study of abrasion-corrosion of AISI 304L austenitic stainless steel in saline solution using acoustic emission technique. NDT E Int. 2000, 33, 363–371, doi:10.1016/S0963-8695(99)00061-4.
22. Mazille, H.; Rothea, R.; Tronel, C. An acoustic emission technique for monitoring pitting corrosion of austenitic stainless steels. Corros. Sci. 1995, 37, 1365–1375, doi:10.1016/0010-938X(95)00036-J.
23. Fregonese, M.; Idrissi, H.; Mazille, H.; Renaud, L.; Cetre, Y. Initiation and propagation steps in pitting corrosion of austenitic stainless steels: Monitoring by acoustic emission. Corros. Sci. 2001, 43, 627–641, doi:10.1016/S0010-938X(00)00099-8.
24. Darowicki, K.; Mirakowski, A.; Krakowiak, S. Investigation of pitting corrosion of stainless steel by means of acoustic emission and potentiodynamic methods. Corros. Sci. 2003, 45, 1747–1756, doi:10.1016/S0010-938X(03)00021-0.
25. Wu, K.; Jung, W.S.; Byeon, J.W. In-situ monitoring of pitting corrosion on vertically positioned 304 stainless steel by analyzing acoustic-emission energy parameter. Corros. Sci. 2016, 105, 8–16, doi:10.1016/j.corsci.2015.12.010.
26. Kovač, J.; Legat, A.; Zajec, B.; Kosec, T.; Govekar, E. Detection and characterization of stainless steel SCC by the analysis of crack related acoustic emission. Ultrasonics 2015, 62, 312–322, doi:10.1016/j.ultras.2015.06.005.
27. Alvarez, M.G.; Lapitz, P.; Ruzzante, J. Analysis of acoustic emission signals generated from SCC propagation. Corros. Sci. 2012, 55, 5–9, doi:10.1016/j.corsci.2011.08.014.
28. Xu, J.; Wu, X.; Han, E.H. Acoustic emission during pitting corrosion of 304 stainless steel. Corros. Sci. 2011, 53, 1537–1546, doi:10.1016/j.corsci.2011.01.030.
29. Behnia, B.; Dave, E. V.; Buttlar, W.G.; Reis, H. Characterization of embrittlement temperature of asphalt materials through implementation of acoustic emission technique. Constr. Build. Mater. 2016, 111, 147–152, doi:10.1016/j.conbuildmat.2016.02.105.

30. Calabrese, L.; Bonaccorsi, L.; Galeano, M.; Proverbio, E.; Di Pietro, D.; Cappuccini, F. Identification of damage evolution during SCC on 17-4 PH stainless steel by combining electrochemical noise and acoustic emission techniques. Corros. Sci. 2015, 98, 573–584, doi:10.1016/j.corsci.2015.05.063.
31. Piotrkowski, R.; Castro, E.; Gallego, A. Wavelet power, entropy and bispectrum applied to AE signals for damage identification and evaluation of corroded galvanized steel. Mech. Syst. Signal Process. 2009, 23, 432–445, doi:10.1016/j.ymssp.2008.05.006.
32. Zhang, J.; Ma, H.; Yan, W.; Li, Z. Defect detection and location in switch rails by acoustic emission and Lamb wave analysis: A feasibility study. Appl. Acoust. 2016, 105, 67–74, doi:10.1016/j.apacoust.2015.11.018.
33. Morizet, N.; Godin, N.; Tang, J.; Maillet, E.; Fregonese, M.; Normand, B. Classification of acoustic emission signals using wavelets and Random Forests: Application to localized corrosion. Mech. Syst. Signal Process. 2016, 70–71, 1026–1037, doi:10.1016/j.ymssp.2015.09.025.
34. Ryan, M.P.; Williams, D.E.; Chater, R.J.; Hutton, B.M.; McPhail, D.S. Why stainless steel corrodes. Nature 2002, 415, 770.
35. Jirarungsatian, C.; Prateepasen, A. Pitting and uniform corrosion source recognition using acoustic emission parameters. Corros. Sci. 2010, 52, 187–197, doi:10.1016/j.corsci.2009.09.001.
36. Feng, X.; Lu, X.; Zuo, Y.; Zhuang, N.; Chen, D. Electrochemical study the corrosion behaviour of carbon steel in mortars under compressive and tensile stresses. Corros. Sci. 2016, 103, 66–74, doi:10.1016/j.corsci.2015.11.006.
37. N.Popov, B. Corrosion Engineering: Principles and Solved Problems; Elsevier: Amsterdam, 2015;
38. Kim, Y.P.; Fregonese, M.; Mazille, H.; Féron, D.; Santarini, G. Ability of acoustic emission technique for detection and monitoring of crevice corrosion on 304L austenitic stainless steel. NDT E Int. 2003, 36, 553–562, doi:10.1016/S0963-8695(03)00065-3.